Dense electron-hole plasma cooling due to second nonequilibrium-phonon bottleneck in CdS crystallites

S. Juršėnas, G. Kurilčik, and A. Žukauskas*
Institute of Materials Science and Applied Research, Vilnius University, Naugarduko 24, 2006 Vilnius, Lithuania

(Received 1 April 1998)

Quantitative evidence on the existence of a second nonequilibrium-phonon bottleneck for dense electron-hole plasma cooling in a highly excited polar semiconductor is presented. The bottleneck is caused by recurrent fusion of nonequilibrium LO phonons from their decay products (daughter phonons). Carrier cooling was experimentally investigated in CdS, which offers a favorable phonon dispersion. Crystallites of 50-nm radius were utilized to prevent stimulated recombination and diffusion of photoexcited electron-hole plasma with a density around 1.5×10^{19} cm^{-3}. A transient of carrier effective temperature, deduced from time-resolved luminescence spectra, exhibit a slow-relaxation component with the time constant of 70 ps at room temperature. The transient was shown to be in quantitative consistence with the theoretical model based on Boltzmann equations for two generations of nonequilibrium phonons and degenerate-carrier energy rate equation with the energy income due to recombination effects (nonradiative capture via multiphonon emission, fermion self-heating, and band-gap renormalization) taken into account. The observed cooling rate agrees with two nonequilibrium-phonon bottlenecks with the depopulation time constants deduced from the available Raman data (0.5 ps for LO phonons and 12.4 ps for daughter phonons). [S0163-1829(98)08543-9]

I. INTRODUCTION

In highly excited semiconductors, nonequilibrium phonons emitted via intraband transitions of hot carriers can be reabsorbed. After carrier quasithermalization to distribution with the effective temperature T, relaxation of the carrier mean energy thus may slow down to a degree determined by the rate of anharmonic depopulation of the nonequilibrium phonons, i.e., by hot-phonon ''cooling.'' The depopulation of nonequilibrium optical phonons takes place on the time scale of ~1 ps at room temperature,[1] which is much larger than that due to carrier-phonon interaction (~100 fs).[2] This effect, designated as ''nonequilibrium phonon bottleneck,'' is widely accepted, especially in polar direct-gap crystals, where long-range Fröhlich carrier-phonon coupling results in efficient amplification of LO vibrations in the central part of the Brillouin zone, which contains small amount of modes.[3–6]

Under extreme levels of photoexcitation, even slower cooling of carriers (~100 ps) was observed in GaAs,[7] GaSe,[8] CdSe,[9] CdS,[10] and $Cd_xS_{1-x}Se$.[11] Initially, some data was accounted for by a crude approximation of screening of the carrier-phonon coupling, which was based on tentative estimations performed in Ref. 12. Later, the experimental data was shown to be in line with a simple balance-equation model of two generations of nonequilibrium phonons each embracing a compact region of the **k** space.[11,13] The first generation of nonequilibrium phonons, i.e., those directly produced by hot carriers, reside within the zone-center region of the LO branch. The second-generation (daughter) ones, produced via anharmonic decay of the nonequilibrium LO phonons, are supposed to excite a certain spherical layer of the **k** space around the wave number of phonons with a half LO-phonon frequency. The long-lived nonequilibrium daughter phonons hinder the depopulation of nonequilibrium LO phonons via recurrent fusion, thus additionally slowing the carrier cooling (second nonequilibrium-phonon bottleneck). However, by using a detailed description of nonequilibrium phonons of two generations in each cell of the reciprocal space, Král and Hejda[14,15] have shown that the nonequilibrium daughter phonons rapidly fuse to the capacious short-wavelength region of the ''mother'' LO branch. They came to a conclusion that this relaxation route results in a negligible heating of the daughter phonons, and, therefore, only first nonequilibrium-phonon bottleneck is substantial for carrier cooling. After all, recently we have demonstrated[16] that this is true only for moderate carrier densities utilized in Refs. 14 and 15. Actually, for hot-carrier densities above 10^{19} cm^{-3}, the short-wavelength region of the LO branch may also be brought out of thermal equilibrium. Moreover, certain peculiarities of the vibration spectra may result in elimination of the zone-boundary modes from the nonequilibrium-phonon interplay. Additionally, the manifestation of the second bottleneck can be considerably enhanced by effects of recombination heating in degenerate-fermion system[17] and by LO-phonon production due to carrier capture by deep centers via multiphonon emission (MPE). Below we present first experimental evidence of slow carrier cooling, which is in quantitative agreement with the extended model of Ref. 16.

The structure of the rest of the paper is as follows. In Sec. II, we ground our selection of CdS crystallites as a model system for observation of the second bottleneck and briefly describe the experimental setup. Then the luminescence spectra and deduced transients for the carrier effective temperature and for other parameters required to estimate the electron-hole plasma (EHP) density are presented. In Sec. III, we outline our theoretical scheme. Section III A contains basic kinetic equations of the model describing the variation of the effective temperature for dense EHP. The plasma density being of crucial importance for slow cooling, the details of the carrier recombination rate in large nanocrystals are described in Sec. III B. In Sec. IV, we show an application of our numerical approach to the experimental data and discuss

 ©1998 The American Physical Society

the reliability of the fitting parameters. Finally, in Sec. V we summarize the results and present our view of the applicability of the second-bottleneck model in other conditions.

II. EXPERIMENTAL PROCEDURE AND RESULTS

The most convenient way to experimentally observe the peculiarities of the carrier mean-energy relaxation is to trace the temporal evolution of the carrier effective temperature after the photoexcitation by a short pulse. A simple insight into EHP transient behavior is offered by time-resolved luminescence spectroscopy. To quantitatively identify the second bottleneck, experimental conditions must provide facilities to define the carrier density with minimal ambiguity. However, the required density regime ($n > 10^{19}$ cm^{-3}) implies degeneracy of the electron-hole plasma even at effective temperatures elevated high above the room temperature. In a crystal with one or more extended dimensions, this invokes stimulated emission and enhanced diffusivity which are difficult to control. Therefore, a quasi-zero-dimensional semiconductor specimen was chosen as the most favorable investigation object, in which the carrier density is homogeneous and predominantly determined by the rates of photogeneration and spontaneous recombination. Such crystallites of nanometer dimensions are extensively investigated because of their unique optical properties related with carrier or/and exciton confinement.[18] However, here these objects were utilized as nothing but small bulklike containers of hot and dense EHP.[19] In the present work, ''large'' CdS nanocrystals embedded in a multicomponent glass matrix were used. The sample, which was fabricated by Ekimov,[20] contained crystallites with the average radius $a = 50$ nm. The crystallite size was small enough to ensure homogeneous photoexcitation via one-photon process (the absorption length for the incident light with the photon energy of 3.50 eV is ~ 100 nm). On the other hand, it was sufficiently large to neglect quantum confinement effects (the exciton Bohr radius is 3 nm in CdS) and to prevent small-size-induced breakdown of **k**-selection rules for electronic transitions (the inverse average wave number of electrons at 300 K is less than 3 nm). Finally, a low density of crystallites in the matrix (1% volume) suggested suppression of stimulated emission because of large diffraction losses.

The sample was excited by using the third harmonics of a passively mode-locked YAG:Nd^{3+} (yttrium aluminum garnet) laser (the duration of the Gaussian pulse is 28 ps, the repetition rate is 2.7 Hz). The experimental results presented below are obtained at the incident density of energy 1.4 mJ/cm^2. With reflectance estimated, this correspond to the averaged power density of 40 MW/cm^2. The secondary emission was temporally resolved by means of a CS_2 optical Kerr shutter, dispersed by a 0.4-m grating monochromator and recorded photoelectrically. To additionally monitor the transient variation of the carrier density, spectrally integrated intensity of each spectra was registered. Before measuring the luminescence spectra, the sample was exposed to several thousand laser shots to stabilize the emission properties by photomodification.[21]

Figure 1 depicts some luminescence spectra obtained at different delay after the excitation pulse. The spectra are seen to contain one emission band with features characteristic of radiative recombination in dense EHP.[22–24] The high-energy region of the spectra reflects the carrier effective temperature. The width of the band can be used for rough estimation of the carrier density, providing that some degeneracy is present and the stimulated emission is negligible. To extract the values of the effective temperature and density, the spectra were fitted with conventional line shapes with the **k**-selection rule for band-to-band transitions taken into account.[24,25] The energy of the renormalized band gap was also determined from the fitting procedure. Points in Fig. 2 show the transient evolution of all obtained parameters. The excess effective temperature [Fig. 2(a)] is seen to reach a value of ≈ 300 K at zero delay and to relax to the equilibrium value with a time constant of about 70 ps. In spite of large errors, the carrier density [Fig. 2(b)] can be asserted to reach the peak values slightly above 10^{19} cm^{-3}, after the excitation pulse is terminated, and to relax on the ~ 100 ps time scale. The variation of the EHP temperature and density makes the renormalized band-gap change in time [Fig. 2(c)]. Kinetics of the luminescence intensity integrated over the spectrum is depicted in Fig. 2(d). After some rise time and nonexponential relaxation, the integrated intensity tends to decay with a time constant of 150 ps.

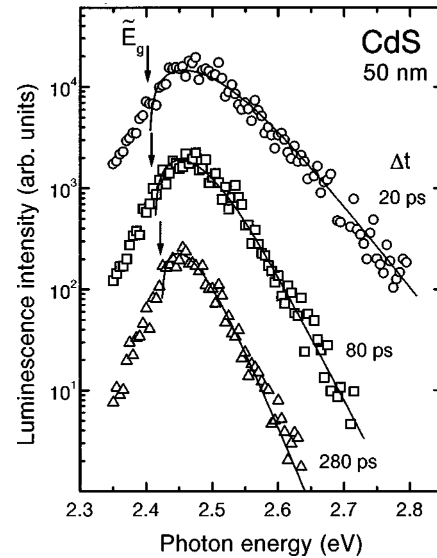

FIG. 1. Transient luminescence spectra of CdS crystallites. The spectra are arbitrarily shifted along the vertical axis. The delay time after the exciting pulse is indicated at each spectrum. Solid lines, approximations by calculated line shapes. Arrows indicate the energy of the renormalized band gap.

III. THEORY

A. Kinetic equations

To simulate a transient of the effective temperature, we employ a kinetic model that starts from the rate equation for total carrier energy per unit volume with conventional concepts of photogeneration, recombination, and carrier-phonon energy exchange taken into account.[3] Below, a brief description of the extended model, which includes Boltzmann equations for occupation numbers of nonequilibrium phonons of two generations,[15] is presented. The description is based on the approach developed in Ref. 16.

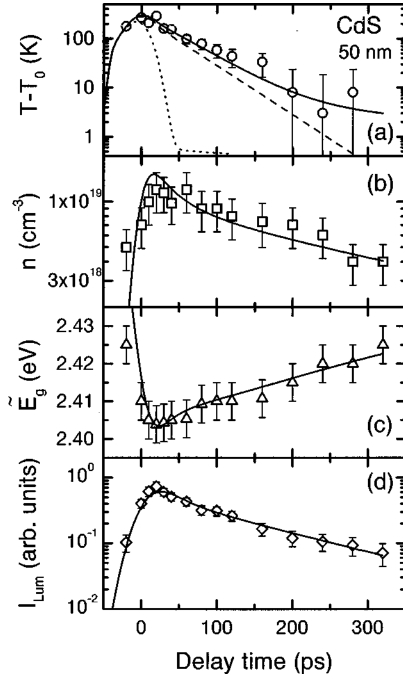

FIG. 2. (a) Temporal evolution of the carrier effective temperature in CdS crystals. Points, experimental values; solid line, result of the numerical simulation; dotted line, same without second nonequilibrium-phonon bottleneck taken into account; dashed line, effect of ''bare'' second bottleneck (recombination-induced effects neglected). (b) Transient behavior of the carrier density. Points, experiment; line, calculation. (c) Same for the renormalized band-gap energy. (d) Transient of the spectrally integrated luminescence intensity. Points, experiment; line, calculation convoluted with the temporal profile of the gate.

It should be noted that when the threshold of the plasma degeneracy is reached, the carrier density becomes comparable with the density of phonon modes the carriers are interacting with. This circumstance results in the emerging of new effects in hot-carrier energy relaxation, which are negligible at moderate carrier density. For instance, at high hot-carrier density, slow recombination-induced variation of fermion *mean* energy[17] may result in significant rate of *total* energy release. This release is capable of maintaining the nonequilibrium occupation numbers of the relevant phonon modes for a time comparable with the carrier lifetime. Again, the nonequilibrium phonons produced via nonradiative recombination of a large amount of carriers may prolong the manifestation of hot-phonon bottlenecks. Here these weak effects are taken into consideration. In the present paper, band-gap renormalization effect is additionally introduced to regard the mean-energy variation caused by carrier interaction.

The carrier mean-energy relaxation and the interplay between two generations of nonequilibrium phonons is considered within an isotropic approximation of electronic and vibration spectra. For simplicity, the holes are treated within a single valence band, thus, the effects due to intervalence-band scattering[5] are neglected. The Brillouin zone is approximated by a sphere of the same volume with the radius q_M. The carriers are assumed to interact with the only one dispersionless LO-phonon branch, and the daughter-phonon branch is supposed to be optical and weakly dispersed within a linear law.[26] The phonon-phonon coupling is assumed to be independent of phonon wave vectors.[15]

Consider temporal variation of the effective temperature for homogeneously photoexcited plasma with the density of the electron-hole pairs n. The exciting pulse is assumed to be long enough for Fermi-Dirac distributions in both electron and hole subsytems to be established with the uniform effective temperature T. Generally, the effective temperature varies in accordance with the variation of the carrier total energy

$$E(n,T)=n\left(\tilde{E}_g+\frac{3}{2}k_BT\sum_i\frac{F_{3/2}(\eta_i)}{F_{1/2}(\eta_i)}\right),\tag{1}$$

where $\tilde{E}_g=\tilde{E}_g(n,T)$ is the renormalized band gap, $\eta_i=\xi_i/k_BT$, and $\xi_i=\xi_i(n,T)$ are the Fermi quasilevels for electrons $(i=e)$ and holes $(i=h)$; $F_j(x)$ is the Fermi integral of the order j. To estimate the band gap renormalization, the results of the partly phenomenological approach[27] were utilized. For carrier temperatures and densities under consideration,

$$\tilde{E}_g=E_g-\frac{\pi^2a_B\kappa}{12}E_R,\tag{2}$$

where E_g is the initial band gap, a_B and E_R are the exciton Bohr radius and Rydberg energy, respectively. The inverse screening length is

$$\kappa=\left(\frac{e^2n}{\varepsilon_0\varepsilon_sk_BT}\sum_i\frac{F_{-1/2}(\eta_i)}{F_{1/2}(\eta_i)}\right)^{1/2},\tag{3}$$

where ε_s is the static dielectric constant.

The rate equation for the carrier total energy is

$$\frac{dE}{dt}=h\nu_{inc}G(t)-\frac{E}{n}R+P_{c\text{-}ph},\tag{4}$$

where $h\nu_{inc}$ is the incident photon energy, G is the carrier photogeneration rate, and R is the recombination rate. Here, each recombination event is assumed to remove the average energy E/n from the system. The third term on the right-hand side of Eq. (4) is the ordinary power of the carrier-phonon exchange, which is obtained by summing the rates of LO-phonon production by carriers[28] over all phonon modes with the wave numbers q. Screening of carrier-phonon coupling was taken into account in the static limit of random-phase approximation by reduction of the relevant rate constants by a factor $[1+(\kappa q)^{-2}]^2$. The power of the carrier-phonon exchange depends on carrier density and effective temperature as well as on mean occupation numbers of LO phonons ν_q.

Comparison of Eqs. (4) and (1) in the manner used in Ref. 17 yields

$$\frac{dT}{dt}=\left(\frac{\partial E}{\partial T}\right)^{-1}\left[\left(h\nu_{inc}-\frac{\partial E}{\partial n}\right)G(t)-\left(\frac{\partial E}{\partial n}-\frac{E}{n}\right)R+P_{c\text{-}ph}\right].\tag{5}$$

Here the partial derivatives on temperature and density are obtained by explicit differentiation of Eq. (1). The first term in the brackets of the right-hand side of Eq. (5) is the energy income rate due to carrier-pair generation by photons and the second one is the power released during the recombination.

The magnitude and the sign of the latter is determined by the competitive variation of the gap width and the mean kinetic energy of the electron-hole pairs with carrier density and effective temperature. For instance, when the carrier density is decreasing, the relevant drop of the Fermi quasilevels increases the effective temperature,[17] while the band gap widens at the expense of the reduction of kinetic energy.

The LO-phonon occupation numbers, which determine the power $P_{c\text{-}ph}$, are assumed to vary in accordance with the Boltzmann equation

$$\frac{d\nu_q}{dt}=\left(\frac{\partial\nu_q}{\partial t}\right)_c+\left(\frac{\partial\nu_q}{\partial t}\right)_N+\left(\frac{\partial\nu_q}{\partial t}\right)_{nr}, \tag{6}$$

where the first term on the right-hand side is the phonon production rate due to carrier intraband transitions.[28] The second term is the rate due to the three-phonon anharmonic interaction with the ensemble of daughter phonons characterized by wave numbers Q and mean occupation numbers N_Q. For daughter phonons with the frequency differing little from half of LO phonon frequency ω_0

$$\left(\frac{\partial\nu_q}{\partial t}\right)_N=-\frac{1}{\vartheta_0(0)Q_S^2 q}\int_{Q_S-\tilde{q}/2}^{Q_S+\tilde{q}/2}Q(2Q_S-Q)\times[\nu_q(1+N_Q+N_{2Q_S-Q})-N_QN_{2Q_S-Q}]\,dQ \quad \text{at } q<2Q_S, \tag{7}$$

where Q_S is the daughter-phonon wave number at the subharmonic frequency $\Omega_{Q_S}=\omega_0/2$, and $\vartheta_0(0)$ is the zero-temperature zone-center LO phonon lifetime. The integration interval is $\tilde{q}=\min[q,2(q_M-Q_S)]$. The energy and momentum conservation yield zero rate at $q>2Q_S$. Assuming that the phonons of higher generations are almost in equilibrium, the occupation numbers of the daughter phonons obey the Boltzmann equation

$$\frac{dN_Q}{dt}=\left(\frac{\partial N_Q}{\partial t}\right)_\nu-\frac{N_Q-N_Q^{(0)}}{\Theta_Q(T_0)}, \tag{8}$$

where $N_Q^{(0)}$ is the equilibrium occupation number, $\Theta_Q(T_0)$ is the characteristic time constant of the anharmonic relaxation to lower-frequency phonons at the ambient temperature. The daughter-phonon production rate due to the three-phonon process involving LO phonons is

$$\left(\frac{\partial N_Q}{\partial t}\right)_\nu=-\frac{2(2Q_S-Q)}{\vartheta_0(0)Q_S^2 Q}\int_{2|Q_S-Q|}^{\tilde{Q}}q\times[N_QN_{2Q_S-Q}-\nu_q(1+N_Q+N_{2Q_S-Q})]\,dq \quad \text{at } 2Q_S-q_M<Q<2Q_S, \tag{9}$$

where $\tilde{Q}=\min(q_M,2Q_S)$. Again, zero rate is obtained for $Q>2Q_S$ and $Q<2Q_S-q_M$. The integration limits in Eqs. (7) and (9) are seen to be determined by the subharmonic wave number Q_S, which is of crucial importance for the manifestation of second bottleneck.[16] At $Q_S>q_M/2$, LO phonons decay to short-wavelength daughter phonons, which can rapidly fuse to numerous modes of zone-boundary LO phonons. Meanwhile, at $Q_S<q_M/2$, the zone-boundary modes are eliminated from the nonequilibrium-phonon interplay, and the second-bottleneck effect considerably increases.

The third term on the right-hand side of Eq. (6) is the rate of the LO-phonon production due to nonradiative recombination of the carriers. In semiconductors with strong electron-phonon coupling, the dominating route of the nonradiative recombination is carrier trapping to deep centers via MPE.[29] Generally, the relaxation of deep traps involves interaction of local vibrations with phonons.[30] However, in undoped semiconductors like CdS, the deep traps originate predominantly from the ''native'' defects (e.g., vacancies) which are known to change the local density of phonon modes rather than to produce local vibrations.[31] Therefore, the nonequilibrium LO phonons can be assumed to be produced directly during the relaxation of the trap. Given that the probability of nonequilibrium phonon emission in a mode q is proportional to its contribution to the Huang-Rhys factor, the relevant phonon production rate is

$$\left(\frac{\partial\nu_q}{\partial t}\right)_{nr}=\frac{n}{\tau_c}\frac{\tilde{E}_g}{\hbar\omega_0}\frac{2\pi^2}{q_Tq^2[1+(\kappa q)^{-2}]^2},\quad q\leqslant q_T, \tag{10}$$

where τ_c is the carrier lifetime and $q_T\cong\pi/a_T$ is the radius of the **k**-space region in which the nonequilibrium LO phonons are produced (a_T is the radius of the trap). Equation (10) implies the domination of the screened Fröhlich coupling.

B. Carrier recombination in crystallites

Equation (5) implies that the carrier density variation rate is

$$\frac{dn}{dt}=G(t)-R. \tag{11}$$

Under homogeneous excitation, the generation rate is $G(t)=\alpha I_{inc}(t)/h\nu_{inc}$, where α is the absorption coefficient and $I_{inc}(t)$ is the incident power density with the relevant temporal profile.

For spherical nanocrystals that exhibit enhanced surface-to-volume ratio, the recombination rate should contain additional terms in comparison with bulk crystals

$$R=R_b+R_s+R_{eh}+R_{pi}. \tag{12}$$

Here the first and the second terms on the right-hand side are the bulk and the surface rates of carrier nonradiative capture via effective-temperature activated MPE, respectively, the third term originates from spontaneous direct band-to-band transitions,[32] and the last one is due to crystallite photoionization effect, which results in carrier trapping in the glass matrix.[33,34] We neglect the Auger recombination as there are no reasonable conditions for its manifestation in bulk CdS,[35] meanwhile, the crystallites under consideration are too large for small-size-enhanced Auger process.[36]

In the high-temperature limit, the bulk nonradiative capture due to MPE is described by Arrhenius probability of surmounting a certain barrier W_b. In strongly polar semiconductors, under conditions of carrier and long-wavelength LO phonon heating, the relevant recombination rate can be ex-

pressed through the effective temperature and equilibrium-temperature lifetime[24] $\tau_b(T_0)$,

$$R_b=\frac{n}{\tau_b(T)}=\frac{n}{\tau_b(T_0)}\left(\frac{T_0}{T}\right)^{3/2}\exp\left[\frac{W_b}{k_BT_0}\left(1-\frac{T_0}{T}\right)\right]. \quad (13)$$

The surface recombination rate can be presented in the similar way[37]

$$R_s=\frac{3S(T)n}{a}=\frac{3S(T_0)n}{a}\left(\frac{T_0}{T}\right)^{3/2}\exp\left[\frac{W_s}{k_BT_0}\left(1-\frac{T_0}{T}\right)\right], \quad (14)$$

where $S(T_0)$ is the equilibrium-temperature surface recombination velocity and W_s is the localization barrier height for dominating centers of capture via MPE on the surface. Both bulk and surface routes of nonradiative capture via MPE are assumed to produce nonequilibrium LO phonons and are taken into account in Eq. (10) through $\tau_c=n/(R_b+R_s)$.

The photoionization effect in Eq. (12) is considered as incident-photon assisted trapping of electrons, localized at the glass-semiconductor interface, to the glass states. For spherical crystallites, the relevant rate is

$$R_{pi}=\frac{3\varrho_s\sigma_{pi}}{a}I\approx b_{pi}G(t), \quad (15)$$

where ϱ_s is the surface density of the filled traps and σ_{pi} is the photoionization cross section. At high excitation intensities, it is reasonable to assume that the surface traps are saturated by electrons due to rapid trapping process,[38,39] therefore, the photoionization rate is proportional to the generation rate and can be expressed as $R_{pi}=b_{pi}G(t)$, where b_{pi} is a certain constant—the photoionization factor ($0\leq b_{pi}<1$).

IV. DISCUSSION

The material-parameter set used in the calculations was that of CdS used in Refs. 11 and 16. Zero-temperature LO-phonon lifetime $\vartheta_0(0)=2.1$ ps was deduced from a precise value of the Raman linewidth.[40] Following the "ω^{-5}" rule,[41] the subharmonic-phonon lifetime of 67 ps at $T_0=0$ was estimated. The extrapolated value of room-temperature depopulation time of subharmonic phonons[16] $\Theta_{Q_S}=12.4$ ps was used for all Q. Experimental values of the carrier bulk lifetime $\tau_b(T_0)=860$ ps, surface recombination velocity $S(T_0)=1300$ cm/s, and localization barrier heights $W_b=200$ meV and $W_s=130$ meV were used.[19,37] The radius of the deep centers for capture via MPE was equaled to one lattice constant.

To fit the experimental data on effective-temperature evolution, the rate equation for the effective temperature [Eq. (5)] was solved in combination with the balance equation for carrier density [Eq. (11)] and a set of the Boltzmann equations for the LO phonons [Eq. (6)] and the daughter phonons [Eq. (8)]. The phonon system was treated discretely by splitting the zone into 100 spherical layers of uniform thickness. The resultant system of 202 differential equations was solved numerically.

The fitting procedure was performed by adjusting three parameters (the absorption coefficient α, the subharmonic wave number Q_S, and the photoionization factor b_{pi}) and by keeping the transient of the carrier density close to the experimental one [Fig. 2(b)]. Solid curve in Fig. 2(a) present the result of simulation at $\alpha=3.3\times10^4$ cm^{-1}, $Q_S=0.18q_M$, and $b_{pi}=0.62$. The curve is seen to completely account for the experimental points. Curves in Figs. 2 from (b) to (d) depict the calculated transients for the carrier density, renormalized band gap, and luminescence intensity ($I_{Lum}\propto R_{eh}$), respectively.

The dotted line in Fig. 2(a) presents the results of simulation obtained at zero lifetime of daughter phonons, i.e., with neglect of the second bottleneck. The transient, which is determined by screening of the carrier-phonon coupling and nonequilibrium LO phonons ($\vartheta_0\approx0.5$ ps at room temperature) is seen to differ negligibly from the shape of 28-ps excitation pulse. Only when the excess effective temperature drops below 1 K, the cooling slows down. The weak residual heating is maintained by total energy release due to recombination-induced effects (variation of fermion mean kinetic energy, band-gap renormalization, and nonradiative recombination). The dashed line in Fig. 2(a) reflects the action of the "bare" second bottleneck, i.e., cooling without the recombination effects [the second term in the brackets on the right-hand side of Eq. (5) and the last term on the right-hand side of Eq. (6) are neglected]. The combined action of all factors (solid curve) infers that weak recombination-induced processes result in a noticeable enhancement of the slow-cooling component caused by the second nonequilibrium-phonon bottleneck.

The calculated evolution of the carrier density [Fig. 2(b)] is in reasonable agreement with the experimental data. Some discrepancy at the peak is probably caused by finite temporal resolution which suggests that the luminescence spectra at zero delay time are contributed by emission of low-density plasma at negative delay time.

The shape of the calculated band-gap transient [Fig. 2(c)] also agrees with the experimental points. However, the fit employs the width of the initial band gap $E_g=2.470$ eV, which is about 15 meV below the actual value obtained from the exciton position at room temperature.[42] This discrepancy may be attributed to a systematic error following from the application of a simplified line shape in describing the low-energy wing of the experimental spectra (Fig. 1).

The calculated transient for the integrated luminescence intensity [Fig. 2(d)] does not explicitly depend on the fitting parameters and just corroborates the set of recombination constants determined in Ref. 37.

The obtained values of the fit parameters are to be discussed. First, it should be emphasized that the value of the absorption coefficient at 3.50 eV (3.3×10^4 cm^{-1}) is in fair agreement with the measured optical density in the same CdS-doped glasses,[43] which yield $\alpha=(2-5)\times10^4$ cm^{-1}. This means that the initial energy passed to the carrier-phonon system in the calculation conforms with the actual energy income caused by the photoexcitation.

The value of the subharmonic wave number ($0.18q_M$) can be compared with those determined by other methods. For instance, the vibrational spectrum of CdS determined by means of small-angle x-ray diffraction[44] yields $Q_S=0.4q_M$ in the B_1 optical branch (Δ direction) which is in line with the second-order Raman measurements.[45] The roughly aver-

aged over directions value of the subharmonic wave number in the B_1 vibration branch described in Ref. 26 is around $0.3q_M$.[11] Recent experimental investigations of inelastic neutron scattering in ^{114}Cd-enriched CdS infer[46] that the B_1 branch exhibits negative group velocity but resides a little bit below the half of LO-phonon frequency (a systematic error, which diminishes the zone-center optical-phonon frequencies, is admitted by the authors of Ref. 46, however). The total combination of the available data indicates that our effective value of the subharmonic wave number is within reasonable limits. Probably, the subharmonic wave number in CdS is less than half of the radii of the zone, indeed. This prevents the daughter phonons from fusing into zone-boundary LO phonons and ensures the most favorable conditions for the observation of second nonequilibrium-phonon bottleneck in carrier cooling.[16]

The third fitting parameter—the photoionization factor is free. It reflects the experimental fact that a significant portion of photogenerated carriers (more than a half in our case) disappears from the nanocrystal during the action of the pump pulse. Although there is a lot of implications for similar behavior of carrier system in nanocrystals,[47,48] the physical meaning of the factor b_{pi} and the way of its introduction should be considered as tentative.

Despite some ambiguities in fit parameters, our approach, which is based on inclusion of conventionally weak factors in energy transfer (fermion recombination heating, nonradiative trapping, band-gap renormalization, and second nonequilibrium-phonon bottleneck), is capable of accounting for the observed slow carrier cooling in a direct-gap semiconductor under high photoexcitation at room temperature. Under experimental conditions employed, the principal role that determines the occurrence of a noticeable slow component in carrier cooling is to be attributed to second nonequilibrium-phonon bottleneck.

V. CONCLUSIONS

We have presented first experimental evidence on slow carrier cooling, which is consistent with the model of two generations of nonequilibrium phonons described by Boltzmann equations.[15,16] By using a specially selected sample and additional transients (for width, position, and intensity of the luminescence band) we have achieved a quantitative agreement of the experimental carrier-cooling kinetics with the model calculations. It should be noted that no adjustment for phonon lifetimes was performed, but the values extrapolated from the Raman linewidth were utilized. These results make possible to claim that the understanding of the second bottleneck has undergone a leap similar to that of the first nonequilibrium-phonon bottleneck in highly excited semiconductors: from pioneer idea of van Driel[49] to quantitative description by Pötz and Kocevar.[3]

The presented results refer to the excitation densities which are more than one order below the threshold of crystal damage. At higher excitation, the cooling time constant may attain values of several hundred ps,[11] i.e., becomes close to carrier lifetime. Probably, this is due to increased role of recombination effects. For instance, under domination of stimulated transitions, which remove electron-hole pairs with the kinetic energy close to zero, Eqs. (4) and (5) suggest a dramatic increase of fermion recombination heating. However, a quantitative analysis of the relevant experimental data may be complicated by ambiguities in describing carrier recombination.

Possible manifestation of second bottleneck in some other materials is of interest. The situation in CdSe is to be similar to that in CdS. In GaAs, where the low-temperature LO phonon lifetime is 7 ps,[50] extrapolation yields that, at room temperature, the daughter phonons should decay to lower-frequency phonons within 40 ps. Thus, second bottleneck can account for some experimental data on slow cooling.[7,51] However, the phonon dispersion curves in GaAs as well as in most cubic crystals infer that the daughter phonons are created in the acoustic LA branch and the subharmonic wave number exceeds a half of the zone radius. As it was mentioned, this involves into interplay numerous modes at zone-boundary,[16] and reduces the daughter-phonon lifetime,[15] unless the zone-boundary phonons come out of equilibrium (some modification of the present model should be performed with a glance to phonon dispersion[15]). Eventually, at the slow stage of the relaxation, the magnitude of the excess effective temperature should be smaller. As for GaN, where the phonon dispersion exhibit zero density of states at half LO phonon frequency both for cubic[52] and hexagonal[53] modifications, the treatment of the energy relaxation via second nonequilibrium-phonon bottleneck requires the LO phonon decay route to be considered in a different way.[54]

ACKNOWLEDGMENTS

The work was supported by the Lithuanian State Science and Studies Foundation. The authors acknowledge the technical support from EKSMA Co. Lasers, Optics, Electronics.

*Electronic address: arturas.zukauskas@ff.vu.lt

[1] E. D. Grann, K. T. Tsen, and D. K. Ferry, Phys. Rev. B **53**, 9847 (1996).

[2] J. A. Kash, J. C. Tsang, and J. M. Hvam, Phys. Rev. Lett. **54**, 2151 (1985).

[3] W. Pötz and P. Kocevar, Phys. Rev. B **28**, 7040 (1983).

[4] U. Hohenester, P. Supancic, P. Kocevar, X. Q. Zhou, W. Kütt, and H. Kurz, Phys. Rev. B **47**, 13 233 (1993).

[5] S. S. Prabhu, A. S. Vengurlekar, S. K. Roy, and J. Shah, Phys. Rev. B **51**, 14 233 (1995).

[6] P. Langot, N. Del Fatti, D. Christofilos, R. Tommasi, and F. Vallèe, Phys. Rev. B **54**, 14 487 (1996).

[7] R. J. Seymour, M. R. Junnarkar, and R. R. Alfano, Solid State Commun. **41**, 657 (1982).

[8] S. S. Yao and R. R. Alfano, Phys. Rev. B **26**, 4781 (1982).

[9] M. R. Junnarkar and R. R. Alfano, Phys. Rev. B **34**, 7045 (1986).

[10] R. Baltramiejūnas, A. Žukauskas, V. Latinis, and S. Juršėnas, Pis'ma Zh. Éksp. Teor. Fiz. **46**, 67 (1987) [JETP Lett. **46**, 80 (1987)].

[11] A. Žukauskas and S. Juršėnas, Phys. Rev. B **51**, 4836 (1995).

[12] E. J. Yoffa, Phys. Rev. B **23**, 1909 (1981).

[13] S. Juršėnas, A. Žukauskas, and R. Baltramiejūnas, J. Phys.: Condens. Matter **4**, 9987 (1992).

[14] K. Král and B. Hejda, Phys. Status Solidi B **174**, 209 (1992).

[15] B. Hejda and K. Král, Phys. Rev. B **47**, 15 554 (1993).
[16] A. Žukauskas, Phys. Rev. B **57**, 15 337 (1998).
[17] D. Bimberg and J. Mycielski, Phys. Rev. B **31**, 5490 (1985).
[18] U. Woggon, in *Optical Properties of Semiconductor Quantum Dots*, edited by G. Höhler, J. Kühn, T. Müller, R. D. Peccei, F. Steiner, J. Trümper, and P. Wölfle, Springer Tracts in Modern Physics Vol. 136 (Springer-Verlag, Berlin, 1997).
[19] S. Juršėnas, V. Stepankevičius, M. Strumskis, and A. Žukauskas, Semicond. Sci. Technol. **10**, 302 (1995).
[20] A. Ekimov, J. Lumin. **70**, 1 (1996).
[21] C. Flytzanis, D. Ricard, and M. C. Shanne-Klein, J. Lumin. **70**, 212 (1996).
[22] H. Yoshida, H. Saito, S. Shionoya, and V. B. Timofeev, Solid State Commun. **33**, 161 (1980).
[23] H.-E. Swoboda, M. Sence, F. A. Majumder, M. Rinker, J.-Y. Bigot, J. B. Grun, and C. Klingshirn, Phys. Rev. B **39**, 11 019 (1989).
[24] S. Juršėnas, G. Kurilčik, and A. Žukauskas, Phys. Rev. B **54**, 16 706 (1996).
[25] Y. Yoshikuni, H. Saito, and S. Shionoya, Solid State Commun. **32**, 665 (1979).
[26] M. A. Nusimovici, M. Balkanski, and J. L. Birman, Phys. Rev. B **1**, 595 (1970).
[27] L. Bányai and S. W. Koch, Z. Phys. B **63**, 293 (1986).
[28] Sh. M. Kogan, Fiz. Tverd. Tela (Leningrad) **4**, 2474 (1962) [Sov. Phys. Solid State **4**, 1813 (1963)].
[29] C. H. Henry and D. V. Lang, Phys. Rev. B **15**, 989 (1977).
[30] V. A. Kremerman, M. Lax, S. G. Demos, D. M. Calistru, and R. R. Alfano, Phys. Rev. B **56**, 14 391 (1997).
[31] M. Lannoo and J. C. Bourgoin, in *Point Defects in Semiconductors I, Theoretical Aspects*, edited by M. Cardona, Springer Series in Solid State Sciences Vol. 22 (Springer-Verlag, Berlin, 1981), Chap. 5.
[32] A. Mooradian and H. Y. Fan, Phys. Rev. **148**, 873 (1966).
[33] V. Ya. Grabovskis, Ya. Ya. Dzenis, A. I. Ekimov, I. A. Kudryavtsev, M. N. Tolstoi, and U. T. Rogulis, Fiz. Tverd. Tela (Leningrad) **31**, 272 (1989) [Sov. Phys. Solid State **31**, 149 (1989)].
[34] J. Malhotra, D. J. Hagan, and B. G. Potter, J. Opt. Soc. Am. B **8**, 1531 (1991).
[35] A. Haug, J. Phys. C **16**, 4159 (1983).
[36] D. I. Chepic, Al. L. Efros, A. I. Ekimov, M. G. Ivanov, V. A. Kharchenko, I. A. Kudriavtsev, and T. V. Yazeva, J. Lumin. **47**, 113 (1990).
[37] S. Juršėnas, G. Kurilčik, M. Strumskis, and A. Žukauskas, Appl. Phys. Lett. **71**, 2502 (1997).
[38] U. Woggon, H. Giessen, F. Gindele, O. Wind, B. Fluegel, and N. Peyghambarian, Phys. Rev. B **54**, 17 681 (1996).
[39] V. Klimov, P. Haring Bolivar, and H. Kurz, Phys. Rev. B **53**, 1463 (1996).
[40] T. C. Damen, R. C. C. Leite, and J. Shah, in *Proceedings of the Tenth International Conference on the Physics of Semiconductors*, edited by S. P. Keller, J. C. Hensel, and F. Stern (U.S. Atomic Energy Comm., Oak Ridge, 1970), pp. 735–739.
[41] P. G. Klemens, Phys. Rev. **148**, 845 (1966).
[42] K. A. Dmitrenko, L. V. Taranenko, S. G. Shevel', and A. V. Marinchenko, Fiz. Tekh. Poluprovodn. **19**, 788 (1985) [Sov. Phys. Semicond. **19**, 487 (1985)].
[43] A. I. Ekimov, Al. L. Efros, and A. A. Onushchenko, Solid State Commun. **56**, 921 (1985).
[44] R. P. Purlys, Ph.D. thesis, Vilnius University, 1983.
[45] B. Kh. Bairamov and Z. M. Khashkhozhev, Fiz. Tverd. Tela (Leningrad) **17**, 1358 (1975) [Sov. Phys. Solid State **17**, 874 (1975)].
[46] A. Debernardi, N. M. Pyka, A. Göbel, T. Ruf, R. Lauck, S. Kramp, and M. Cardona, Solid State Commun. **103**, 297 (1997).
[47] T. Okuno, H. Miyajima, A. Satake, and Y. Masumoto, Phys. Rev. B **54**, 16 952 (1996).
[48] E. Vanagas, J. Moniatte, M. Mazilu, P. Riblet, B. Hönerlage, S. Juodkazis, F. Paille, J. C. Plenet, J. G. Dumas, M. Petrauskas, and J. Vaitkus, J. Appl. Phys. **81**, 3586 (1997).
[49] H. M. van Driel, Phys. Rev. B **19**, 5928 (1979).
[50] D. von der Linde, J. Kuhl, and H. Klingenberg, Phys. Rev. Lett. **44**, 1505 (1980).
[51] T. Amand and J. Collet, J. Phys. Chem. Solids **46**, 1053 (1985).
[52] K. Karch, F. Bechstedt, and T. Pletl, Phys. Rev. B **56**, 3560 (1997).
[53] H. Siegle, G. Kaczmarczyk, L. Filippidis, A. P. Litvinchuk, A. Hoffmann, and C. Thomsen, Phys. Rev. B **55**, 7000 (1997).
[54] K. T. Tsen, D. K. Ferry, A. Botchkarev, B. Sverdlov, A. Salvador, and H. Morkoc, Appl. Phys. Lett. **72**, 2132 (1998).